On the mode-coupling theory for the velocity autocorrelation functions of simple liquids

1997 J. Phys.: Condens. Matter 9 11009

(http://iopscience.iop.org/0953-8984/9/50/007)

J. Phys.: Condens. Matter **9** (1997) 11009–11021. Printed in the UK PII: S0953-8984(97)86717-3

On the mode-coupling theory for the velocity autocorrelation functions of simple liquids

Manel Canales†§ and Joan Àngel Padró‡

† Departament de Física i Enginyeria Nuclear, Universitat Politècnica de Catalunya, Mòdul B4, Campus Nord, Sor Eulàlia d'Anzizu s/n, 08034 Barcelona, Spain

‡ Departament de Física Fonamental, Universitat de Barcelona, Diagonal 647, 08028 Barcelona, Spain

Received 11 August 1997

Abstract. The velocity autocorrelation functions and the corresponding memory functions for a set of liquid metals and Lennard-Jones fluids have been calculated using a mode-coupling theory. The data required for the theoretical calculations have been obtained from molecular dynamics simulations. The influence of both the short repulsive wall and the attractive well of the potential on the binary and mode-coupling terms of the memory function has been analysed. The mode-coupling theory has been tested by comparing the theoretical results with those directly obtained from computer simulations. The most marked discrepancies correspond to systems showing velocity autocorrelation functions with weak backscattering. In the case of the Lennard-Jones fluids, the binary term of the memory function is less well described using a gaussian function.

1. Introduction

Molecular dynamics (MD) simulation is a useful technique for computing static and dynamical properties of fluids. Furthermore, MD constitutes a suitable tool for checking the theories of liquids, since some of the properties involved in them cannot be directly obtained from experiments. The velocity autocorrelation function $C(t)$ is an example of such properties. The first MD studies of $C(t)$ for simple liquids were developed around the middle of the 1960s, just when Zwanzig and Mori established their general theory on the projection operators and memory functions for time correlation functions. At the beginning of the 1970s several phenomenological models for $C(t)$ and its memory function $K(t)$ were proposed. A summary may be found in the books of Boon and Yip [1] and Hansen and McDonald [2]. However, some researchers looked for theories based on first principles which gave a complete picture of the $C(t)$ and could explain important features such as the backscattering or the long-time-tail $t^{-3/2}$-behaviour. With that aim, microscopic studies based on generalized kinetic and mode-coupling theories were applied to compute the time correlation functions of simple liquids [1–3]. The Sjögren and Sjölander (SS) theory [4, 5], based on a combination of kinetic and mode-coupling concepts, is one of the most successful approaches. Moreover mode-coupling theories have also been applied to other problems such as that of the dynamical properties of polymeric liquids, the analysis of glass transitions for supercooled liquids, and the determination of the paramagnetic region for magnetic systems or the dynamics of critical phenomena [6, 7].

§ E-mail: canales@fen.upc.es.

0953-8984/97/5011009+13$19.50

The SS theory is based on the hypothesis that $C(t)$ can be divided into two parts: (1) a binary term which is associated with the short-time events and (2) a mode-coupling term which incorporates more sophisticated processes that appear at longer times. This theory has yielded good results for liquid Ar [4] and liquid monovalent metals [8–15] near their triple point. However, some discrepancies have been observed for liquid metals at higher temperatures [13, 16–18]. causes of these discrepancies and the situations in which they appear have not been sufficiently analysed. The main objective of this work is to check the SS theory for a wide variety of simple liquids characterized by $C(t)$s with different shapes. We have also analysed the influence of the different parts of the potential on both the binary and mode-coupling terms. So, we have also considered systems of particles with purely repulsive interactions by truncating the potentials at their first minima.

The paper is organized as follows. In section 2 the SS mode-coupling theory is summarized and the basic formulas are compiled. The computational details as well as the numerical procedures used to calculate the memory function are described in section 3. The results are shown in section 4. The dependences of the mode-coupling and binary terms of the memory function are discussed in section 4.1, whereas section 4.2 is devoted to the comparison of the mode-coupling and molecular dynamics results. Finally, the main conclusions of the work are stated in section 5.

2. Mode-coupling theory

The time correlation functions such as $C(t)$ can be studied through the formalism developed by Zwanzig and Mori, which is based on a Volterra-like integral equation [1–3]:

$$\frac{\mathrm{d}C(t)}{\mathrm{d}t} = -\int_0^t K(t')C(t-t')\,\mathrm{d}t' \tag{1}$$

where $K(t)$ is a more basic property called the memory function.

One of the conclusions of the MD simulation work by Levesque and Verlet [19] on dense Lennard-Jones fluids was that $K(t)$ may be well described by the analytical expression

$$K(t) = A\exp(-at^2) + Bt^4\exp(-bt). \tag{2}$$

Thus, the memory function can be divided into two parts. The first is a gaussian term dominant at short times, which takes into account the single uncorrelated binary collisions. The second term is initially negligible, increases with time as t^4, reaches a maximum and, finally, decays exponentially. This term is related to the collective effects. During the 1970s, several theoretical investigations were developed in order to give physical sense to the previous analytical form. One of these studies was that of Sjögren and Sjölander [4] who, following the results of Levesque and Verlet, divided the memory function into two terms:

$$K^{SS}(t) = K_B(t) + K_{MC}(t) \tag{3}$$

where we have termed the memory function calculated according the Sjögren and Sjölander theory $K^{SS}(t)$. $K_B(t)$ is the binary memory function, whereas $K_{MC}(t)$ is obtained by using the mode-coupling theory [1–3] which is based on the idea that the motion of a tagged particle is influenced by constraints collectively imposed by its neighbouring particles.

2.1. The binary term

Following the Levesque and Verlet results, Sjögren and Sjölander assumed a gaussian functional for the binary term:

$$K_B(t) = \Omega_0^2 \exp(-t^2/\tau^2) \tag{4}$$

where Ω_0^2 is the square of the Einstein frequency or the initial value of the memory function, which can be obtained from the radial distribution function $g(r)$ and the pair potential $\phi(r)$ [1–3]. The parameter τ, which plays the role of an averaged collision time, can be approximately expressed in terms of $g(r)$, the first and second derivatives of $\phi(r)$ and the static structure factor $S(k)$ [3, 4, 8, 15].

2.2. The mode-coupling term

Sjögren and Sjölander considered the coupling of the velocity of a tagged particle with the density and the longitudinal and transverse currents of the system. They assumed that the mode-coupling part has four contributions [4, 8]:

$$K_{MC}(t) = K_{00}(t) + K_{01}(t) + K_{11}(t) + K_{22}(t). \tag{5}$$

The Laplace transforms of these terms are

$$\begin{aligned}
\tilde{K}_{00}(z) &= \tilde{R}_{00}(z) \\
\tilde{K}_{01}(z) &= \tilde{R}_{01}(z)\left[\tilde{K}_B(z) + \tilde{K}^{SS}(z)\right] \\
\tilde{K}_{11}(z) &= \tilde{K}_B(z)\tilde{R}_{11}(z)\tilde{K}^{SS}(z) \\
\tilde{K}_{22}(z) &= \left[\tilde{K}_B(z) + \tilde{R}_{00}(z) + \tilde{K}_B(z)\tilde{R}_{01}(z)\right]\tilde{R}_{22}(z)\tilde{K}^{SS}(z)
\end{aligned} \tag{6}$$

where $\tilde{K}_B(z)$ and $\tilde{K}^{SS}(z)$ are respectively the Laplace transforms of the binary term and the total memory functions. The Laplace transform of this last element is

$$\tilde{K}^{SS}(z) = \frac{\tilde{K}_B(z) + \tilde{R}_{00}(z) + \tilde{K}_B(z)\tilde{R}_{01}(z)}{1 - \tilde{R}_{01}(z) - \tilde{K}_B(z)\tilde{R}_{11}(z) - [\tilde{K}_B(z) + \tilde{R}_{00}(z) + \tilde{K}_B(z)\tilde{R}_{01}(z)]\tilde{R}_{22}(z)} \tag{7}$$

where the $\tilde{R}_{ij}(z)$ are the Laplace transforms of the recollision terms $R_{ij}(t)$ that are compiled in references [4, 3, 8]. The final forms of the $R_{ij}(t)$ quantities, when spherical symmetry is assumed, are

$$\begin{aligned}
R_{00}(t) &= \frac{\rho k_B T}{6\pi^2 m}\int_0^\infty k^4 c^2(k)\,\Delta F_s(k,t)\,F(k,t)\,\mathrm{d}k \\
R_{01}(t) &= -\frac{1}{6\pi^2\Omega_0^2}\int_0^\infty k^2 c(k)\left[\gamma_L(k) + \frac{\rho k_B T}{m}k^2 c(k)\right]\Delta F_s(k,t)\,\frac{\partial F(k,t)}{\partial t}\,\mathrm{d}k \\
R_{11}(t) &= -\frac{1}{6\pi^2\Omega_0^4\rho}\int_0^\infty k^2\left[\gamma_L(k) + \frac{\rho k_B T}{m}k^2 c(k)\right]^2\Delta F_s(k,t)\,\frac{C_l(k,t)}{C_l(k,0)}\,\mathrm{d}k \\
R_{22}(t) &= -\frac{1}{3\pi^2\Omega_0^4\rho}\int_0^\infty k^2\left[\gamma_T(k)\right]^2\Delta F_s(k,t)\,\frac{C_t(k,t)}{C_t(k,0)}\,\mathrm{d}k
\end{aligned} \tag{8}$$

where ρ is the density, m the atomic mass, T the temperature, k_B the Boltzmann constant, $c(k)$ the Fourier transform of the direct correlation function and $\gamma_L(k)$ and $\gamma_T(k)$ two k-dependent quantities which are defined in references [3, 15]. $F(k,t)$ and $F_s(k,t)$ are the intermediate coherent and incoherent scattering functions and $C_l(k,t)$ and $C_t(k,t)$ are the longitudinal and transverse current correlation functions [2, 3]. $\Delta F_s(k,t)$ is the difference

between $F_s(k,t)$ and $F_0(k,t)$, where $F_0(k,t) = \exp(-(k_BT/2m)k^2t^2)$ is the free-particle form of the intermediate-scattering function.

$K_{00}(t)$, which is in general the dominant term, starts like t^4 and incorporates the effects of the coupling of the velocity of a tagged particle with the density fluctuations of the surrounding medium. The $K_{01}(t)$, $K_{11}(t)$ and $K_{22}(t)$ terms start like t^6 and reflect respectively the coupling with the first derivative of the dynamic structure factor, the longitudinal and the transverse currents [8].

3. Computational details

3.1. Interatomic potentials

The results presented in this paper have been obtained from MD simulations of particles with the mass of ^{7}Li by assuming different interaction potentials. Except for run LM1T, systems at the same temperature and density ($T = 470$ K and $\rho = 0.044\,512$ Å^{-3}) which correspond to liquid lithium close to the triple point have been considered. Run LM1T corresponds to liquid Li at $T = 843$ K and $\rho = 0.041\,62$ Å^{-3}.

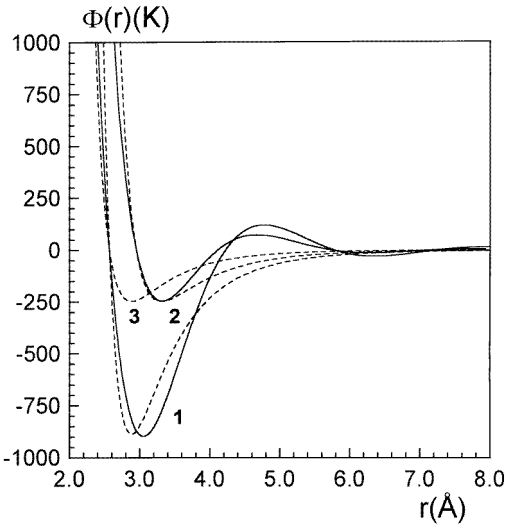

Figure 1. Effective pair potentials. Solid lines: liquid metals (LM1 and LM2); dashed lines: Lennard-Jones systems (LJ1, LJ2 and LJ3).

Two liquid-metal potential models (LM1 and LM2) have been assumed. LM1 is an effective potential for Li with no adjustable parameters, deduced from the neutral-pseudoatom (NPA) method [20]. Since the effective potentials depend on the thermodynamic state, the potential used in the run LM1T is slightly different from LM1, despite the two of them being obtained by the same procedure. However, the differences between LM1 and LM1T are very small. LM2 was obtained by assuming an empty-core pseudopotential with a core radius determined by fitting the calculated main peak of the static structure factor $S(k)$ to the experimental value [21]. Although the shapes of the LM1 and LM2 potential functions are markedly different, they produce similar properties which are in agreement with the available experimental data [22, 23]. As may be observed in figure 1, the LM1 potential shows a deeper potential well at a smaller r-value than the deep well of LM2.

Hence, the mean interatomic distances for LM2 are larger than those for LM1. The volume packing fractions ($\eta = \rho\pi\sigma^3/6$) corresponding to our simulations with LM1 and LM2 are $\eta = 0.4$ and $\eta = 0.6$, respectively. Other effective pair potentials recently used in MD simulations of liquid Li [14, 24] are intermediate between the LM1 and LM2 models but significantly closer to LM1.

Table 1. The position of the first zero (σ) and the depth of the first minimum of the potentials (ϵ), together with the reduced densities (ρ^*) and temperatures (T^*) of the systems simulated in this work.

System	σ (Å)	ϵ (K)	ρ^*	T^*
LM1, RLM1	2.57	887	0.756	0.530
LJ1, RLJ1	2.57	887	0.756	0.530
LM1T	2.57	951	0.706	0.886
LM2, RLM2	2.95	248	1.143	1.895
LJ2, RLJ2	2.95	248	1.143	1.895
LJ3	2.57	248	0.756	1.895

The main features of the potential functions may be simply characterized by two parameters, i.e. the position of the first zero (σ) and the depth of the first minimum (ϵ). The values of σ and ϵ for the different potentials together with the reduced densities ($\rho^* = \rho\sigma^3$) and temperatures ($T^* = k_B T/\epsilon$) of the systems studied in this work are reported in table 1. Balucani *et al* [10] have shown that the properties of different alkali metals (Na, K, Rb and Cs) at states close to the triple point show a common behaviour when reduced units are used. The reduced density and temperature of these systems ($\rho^* = 0.895$ and $T^* = 0.78$–0.84) are intermediate between those for LM1 and LM2. According to these findings, the LM1 and LM2 potentials may be considered as two extreme models representative of liquid alkali metals near the melting point, though the properties of the real systems would be closer to those with LM1.

Lennard-Jones potentials with the same σ and ϵ as LM1 and LM2 have also been considered and they will be termed LJ1 and LJ2, respectively. The reduced densities and temperatures of the systems simulated with these potentials are the same as those corresponding to LM1 and LM2. We have also performed MD simulations of a Lennard-Jones fluid with the same σ as LJ1 and the same ϵ as LJ2. This potential will be termed LJ3. Moreover, four purely repulsive interaction models have been assumed. These potentials, which are termed RLM1, RLM2, RLJ1 and RLJ2, are the same as LM1, LM2, LJ1 and LJ2, respectively, but truncated at their first minima.

3.2. Computer simulations

A cubic box with 668 particles and periodic boundary conditions [25] has been considered in each of the simulations. Beeman's algorithm [26] with a time step of 3 fs has been used for the numerical integration of the equations of motion. The properties of the systems have been determined during runs of 10^5 time steps, after an equilibration period of 10^4 time steps. This study includes the calculation of radial distribution functions, velocity autocorrelation functions, mean square displacements, shear and bulk viscosities and thermal conductivities as well as k-dependent properties such as coherent and incoherent intermediate-scattering functions and longitudinal and transverse current correlation functions. The k-dependent properties have been calculated for 20 different ks within the 0.25 Å^{-1} and 5 Å^{-1} interval.

3.3. Calculation of the memory function

The memory function $K(t)$ has been determined by two procedures. The former is based on the numerical solution of equation (1). To this end, several algorithms have been proposed [27–30]. We have used the method of Berne and Harp [27] to calculate the $K(t)$s from the $C(t)$s resulting from the MD simulations. These memory functions, which may be considered as 'exact' results, will be named $K^{MD}(t)$. The second procedure consists in the calculation of $K(t)$ according to the mode-coupling theory of Sjögren and Sjölander, $K^{SS}(t)$. This method requires the determination of $K_B(t)$ and $K_{MC}(t)$. For this calculation we have used different MD results. The parameters Ω_0 and τ of the binary term (see equation (4)) have been computed from the $g(r)$s. In order to obtain $S(k)$, which is required for the computation of τ, the function $g(r)$ has been extended to distances greater than the half-length of the simulated cubic box using the procedure proposed by Verlet [25, 31]. To this end the Ornstein–Zernicke equation has been solved using the algorithm designed by Zerah [32]. The same procedure has been used to calculate $c(k)$, which is also required for the computation of $K_{MC}(t)$.

The knowledge of the full $F(k,t)$, $F_s(k,t)$, $C_l(k,t)$ and $C_t(k,t)$ functions is needed to compute $K_{MC}(t)$ (see equations (5)–(8)). For this reason we have considered four k-regions and different treatments have been used for each of them.

For $k < 0.25$ Å^{-1} the hydrodynamic model has been assumed. According to this model $S_s(k,\omega)$ and $C_t(k,\omega)$ are single lorentzians centred at $\omega = 0$ and $S(k,\omega)$ is made up of three lorentzians centred at the origin an at $\omega = \pm v_s k$, v_s being the adiabatic velocity of sound [1–3, 33]. The thermodynamic and transport coefficients required to compute these functions have been obtained from the energy and pressure fluctuations [25] and using the Green–Kubo relations [25, 34], respectively.

An interpolation procedure [35] has been applied to the MD results to obtain the correlation functions in the 0.25 Å$^{-1} \leqslant k \leqslant 2$ Å^{-1} interval.

In the 2 Å$^{-1} \leqslant k \leqslant 5$ Å^{-1} region, the functions change sharply and interpolation methods cannot be used. Thus, the viscoelastic model developed by Lovesey [36] has been assumed. It is based on the assumption of an exponential behaviour of the second-order memory function of $F(k,t)$ [3, 36]. The coefficients appearing in the $F(k,t)$ expression can be obtained from the radial distribution function, the pair potential and its derivatives. This model has been checked for different simple liquids [3, 36–38] and in all cases it has yielded good results for ks close to the $S(k)$ maximum. The viscoelastic model for the transverse current correlation function can be constructed by an analogous procedure, but in this case the knowledge of the shear viscosity coefficient η_S and the assumption of a special closure relation, such as that in the Akcasu and Daniels approach, are required [3]. $F_s(k,t)$ has been computed by assuming a gaussian approximation [1–3]:

$$F_s(k,t) = \exp\left[-\tfrac{1}{6}k^2 r^2(t)\right]$$

where $r^2(t)$ is the mean square displacement.

For $k > 5$ Å^{-1} the free-particle approach [2, 3] has been assumed. Thus,

$$F(k,t) = F_s(k,t) = C_t(k,t)/C_t(k,0) = F_0(k,t) = \exp\left(-\frac{k_B T}{2m}k^2 t^2\right)$$

and

$$C_l(k,t)/C_l(k,0) = \left(1 - \frac{k_B T}{m}k^2 t^2\right)\exp\left(-\frac{k_B T}{2m}k^2 t^2\right).$$

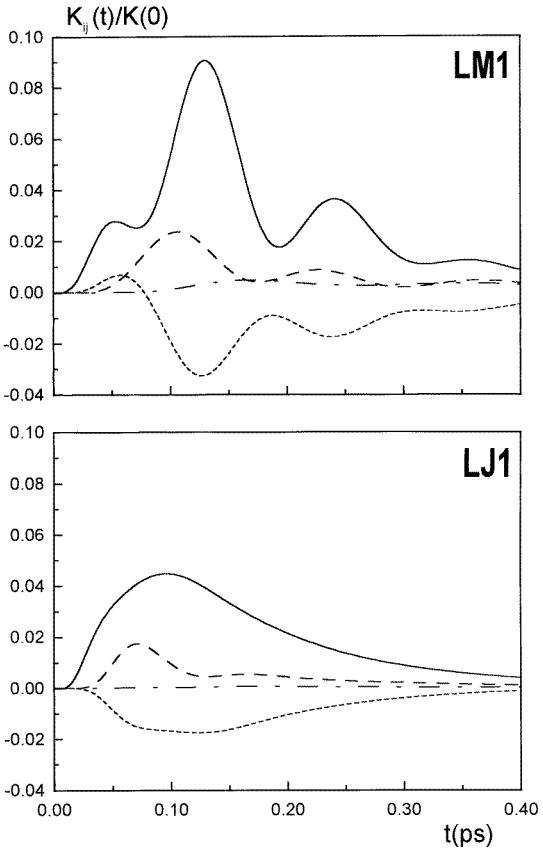

Figure 2. Mode-coupling contributions to the memory for the LM1 and LJ1 systems. Solid lines: $K_{00}(t)$; dashed lines: $K_{01}(t)$; long-dashed lines: $K_{11}(t)$; long-dashed–dotted lines: $K_{22}(t)$. The functions have been normalized with respect to $K_{MD}(0)$.

4. Results

4.1. The mode-coupling term

The four contributions to $K_{MC}(t)$ have been calculated according to the procedure described in the preceding section. As for other simple liquids [8, 11, 13, 16], that of $K_{00}(t)$ is the dominant contribution. Moreover $K_{01}(t)$ and $K_{11}(t)$ are of the same order of magnitude but have opposite signs, whereas the contribution of $K_{22}(t)$, which is the term responsible for the asymptotic $t^{-3/2}$-behaviour of $C(t)$, is negligible in all of the cases considered in this work. In general the $K_{ij}(t)$s for liquid metals are large and show more marked oscillations than those for the Lennard-Jones fluids for the same reduced thermodynamic conditions. The results for LM1 and LJ1 are shown in figure 2.

The density–density contributions to $K_{MC}(t)$ are displayed in figure 3. $K_{00}(t)$ for liquid metals shows three peaks, whereas for Lennard-Jones systems it only shows a low peak. The three peaks may also be clearly observed in the case of the purely repulsive potential RLM2 but for RLM1 they are significantly smoothed. These results indicate that the three-peak structure should be related to the softer repulsive wall of the liquid-metal potentials. The

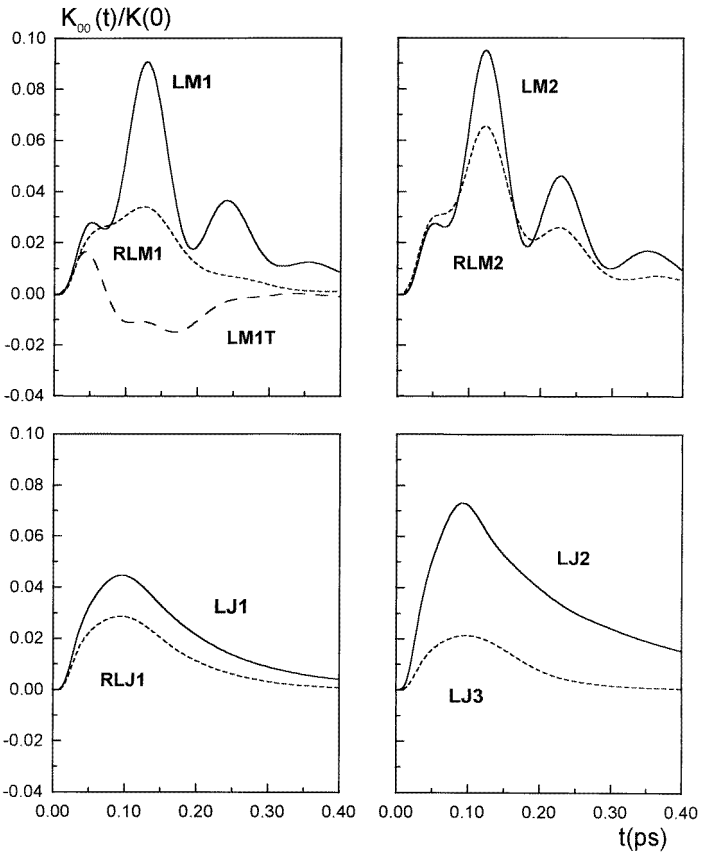

Figure 3. The density–density $K_{00}(t)/K_{MD}(0)$ mode-coupling terms.

interactions at distances beyond the first minima of the potentials have no noticeable effects on the positions of the peaks, but produce a significant increase of the height of the maxima. This increase is more evident for LM1; this may be associated with the stronger attractive forces for this potential. Finally it can be observed that an increase of the temperature gives raise to a decrease of the $K_{00}(t)$ maxima.

4.2. The binary term

The theoretical results for Ω_0^2 and τ calculated from the $g(r)$, $S(k)$ and $\phi(r)$ [1–3] are gathered together in table 2. The differences among the values of Ω_0^2 reflect the differences between the radial distribution functions and the pair potentials for the different systems. The values of τ can be divided in two groups: on the one hand, the liquid metals and their repulsive models; and on the other hand, the Lennard-Jones systems and their respective repulsive interaction systems. This shows that the short-time dynamics is basically dependent on the repulsive wall of the potential. The direct comparison of the results for RLJ1 and RLM1, for which the $g(r)$s are very similar, indicate that softer repulsive walls of the potential produce lower values of Ω_0^2 and higher τ-values. The other parts of the potential increase Ω_0^2 and τ moderately, this increase being larger for potentials with a deeper well. The values of Ω_0^2 for LM1 and LM1T show that this quantity decreases

when the temperature increases. This may be related to the weaker structure of the fluid at high temperature.

Table 2. The square of the Einstein frequency (Ω_0^2), and the theoretical values (τ_{theo}) and fitted values (τ_{fit}) of the averaged collision times of the binary term of the memory function.

System	Ω_0^2 (ps^{-2})	τ_{theo} (ps)	τ_{fit} (ps)
LM1	1673	0.0317	0.0353
RLM1	1520	0.0272	0.0296
LM1T	1598	0.0280	0.0296
LM2	1795	0.0317	0.0351
RLM2	1747	0.0311	0.0329
LJ1	2875	0.0168	0.0177
RLJ1	2869	0.0143	0.0159
LJ2	3737	0.0175	0.0200
RLJ2	3730	0.0181	0.0209
LJ3	1551	0.0185	0.0197

We have also calculated τ by fitting a gaussian function (see equation (4)) to $K_B(t)$ calculated according to the expression $K_B(t) = K^{MD}(t) - K_{MC}(t)$. The fitted τ-values (see table 2) are greater than the theoretical ones, the differences being about 10%–15%. Due to the incomplete description of the binary term using a gaussian function with the values of Ω_0^2 and τ calculated theoretically, some authors assumed a functional form with a softer decay, such as $\mathrm{sech}^2(t/\tau)$ [3, 9, 10, 15]. However, a careful analysis of both functional forms for our systems has shown that the short-time dynamics may be better described by a gaussian function, but with the parameters obtained from the fitting instead of the theoretical values. The fit is more reliable for liquid metals than for Lennard-Jones fluids including the corresponding repulsive models (chi squared for the fit is three orders of magnitude smaller for liquid metals than for Lennard-Jones systems). So, the binary part used for checking the SS theory in the next section is the gaussian functional with the fitted τ-value.

4.3. The velocity autocorrelation function

The resulting $C^{MD}(t)$ functions are compared with their respective $C^{SS}(t)$s in figure 4. In the case of the liquid metals (LM1, LM2 and LM1T) we can observe a good agreement between theoretical and simulation findings. However, there are some discrepancies in the case of the repulsive potential models (specially for RLM1). The disagreements are more marked for the Lennard-Jones systems. It should be noted that these discrepancies in $C(t)$ can produce significant differences between self-diffusion coefficients (about 40% in some cases). In figure 4 we have also represented the $C^{SS}(t)$ functions obtained when the mode-coupling contribution to the memory function is omitted ($K^{SS}(t) \sim K_B(t)$). In general the contribution of the $K_{MC}(t)$ term is rather small. It is interesting to note that in some cases (RLM1, RLJ1 and LJ3) the agreement with the $C^{MD}(t)$ functions is significantly better when only the binary part of the memory function is considered. Our results suggest that the SS theory produces more reliable results for systems with $C(t)$ functions which present more pronounced backscattering. This is consistent with the deficiencies of the SS theory observed for liquid metals at high temperatures [13, 16–18].

In order to analyse more carefully the discrepancies between the MD and the SS results

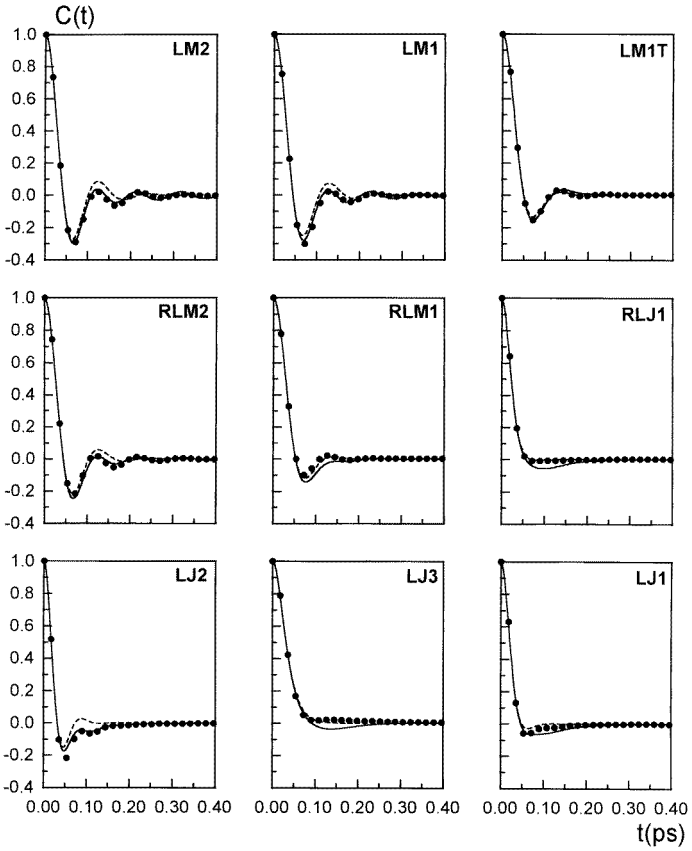

Figure 4. Velocity autocorrelation functions. Dots: $C_{MD}(t)$; solid lines: $C^{SS}(t)$; dashed lines: $C^{SS}(t)$ assuming $K^{SS}(t) = K_B(t)$.

we have calculated

$$\Delta K(t) = \frac{K^{MD}(t) - K^{SS}(t)}{K^{MD}(0)} = \frac{K^{MD}(t) - K_B(t) - K_{MC}(t)}{K^{MD}(0)}. \tag{9}$$

For a more reliable comparison the differences have been normalized with respect to the initial values of $K_{MD}(t)$. The $\Delta K(t)$ results together with the contributions of the binary and mode-coupling terms are shown in figure 5. In general $\Delta K(t)$ shows values of the same order of magnitude as those of $K_{MC}(t)/K^{MD}(0)$. As with the $C(t)$ functions, for some systems (LM1, LM2, LM1T, RLM2 and RLJ2) the contribution of the mode-coupling term diminishes $\Delta K(t)$, and the theoretical $K^{SS}(t)$ functions become improved, but for the other systems, which are characterized by $C(t)$ functions with weak backscattering, the mode-coupling contribution increases $\Delta K(t)$. In relation to the contribution of the binary term to $K^{SS}(t)$ we can observe that in the case of potentials with a soft repulsive wall, such as for liquid metals, the assumed gaussian model produces reasonable results. This is in contrast with the conclusions of Nowotny and Kahl [13], who attributed the failure of the SS theory for the $C(t)$ of a liquid metal at high temperature (with a weak backscattering) to the binary term. However, for the Lennard-Jones systems, with more repulsive potential walls, the $\Delta K(t)$ functions show peaks at short times which indicate that the $K_B(t)$ function

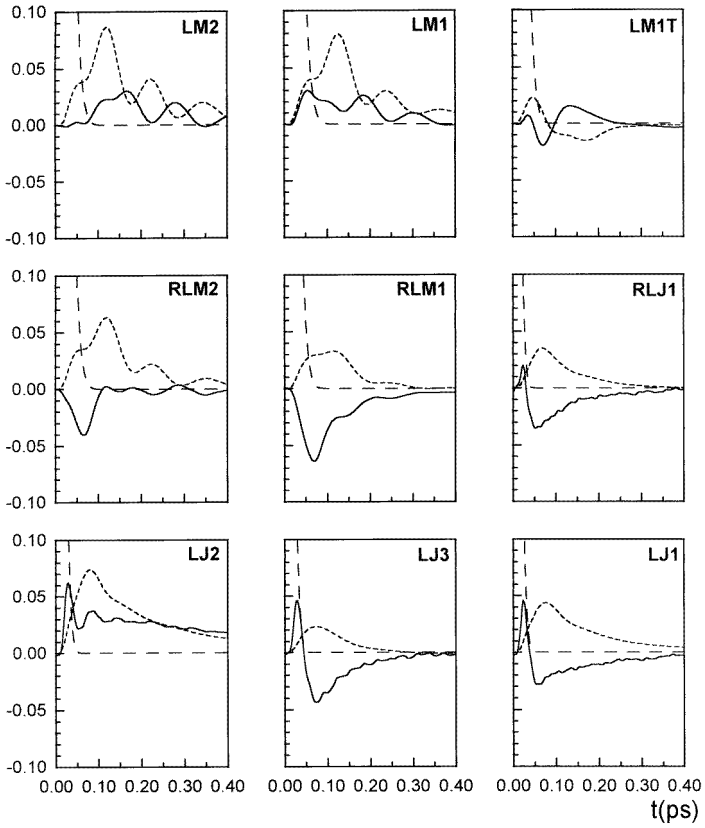

Figure 5. Solid lines: $\Delta K(t) = \left[K^{MD}(t) - K^{SS}(t)\right]/K^{MD}(0)$; long-dashed lines: $K_B(t)/K^{MD}(0)$; dashed lines: $K_{MC}(t)/K^{MD}(0)$.

should be improved. This is consistent with the less accurate fit of the gaussian function to the $K_B(t)$s for these systems.

Gudowski *et al* [16] and Larsson [17] suggested fitting $K(t)$ to a corrected version of the Levesque and Verlet formula:

$$K(t) = A\exp(-at^2) + Bt^4\exp(-bt) - Ct^{\gamma}\exp(-c^2t^2). \tag{10}$$

However, our $\Delta K(t)$ results cannot be reasonably fitted by using this function. The findings in this paper suggest that $\Delta K(t)$ does not take the form of a simple function, and that a modified version of the SS theory should probably be developed. Larsson [17] has already stated that the decomposition of $K(t)$ into two independent terms is unrealistic, and he supported the development of a new theory which incorporates a certain degree of interdependence between the binary and mode-coupling terms. Our results support this idea, since the largest $\Delta K(t)$ values in general correspond to the time interval for which $K_B(t)$ becomes close to zero and $K_{MC}(t)$ starts to increase.

5. Conclusions

The mode-coupling contribution to $K(t)$, which is basically due to the density–density $K_{00}(t)$ term, is larger in liquid metals than in Lennard-Jones fluids under equivalent thermo-

dynamic conditions. In the case of liquid metals, $K_{00}(t)$ shows a three-peak structure while for Lennard-Jones systems there is only one peak. This has been associated with the softer repulsive wall of the former potentials and is more evident for the systems with a high volume packing fraction. The attractive well of the potential increases the heights of the peaks.

The binary term of the memory function is correctly described using a gaussian functional with fitted parameters, especially for liquid metals. The values of Ω_0^2 and τ mainly depend on the repulsive wall of the potential. The lower values of Ω_0^2 and higher values of τ correspond to the softer potential walls. The attractive well of the potential has a minor influence on these parameters.

The SS theory yields good results for dense liquids metals. However, noticeable discrepancies between the MD and SS results have been observed when the $C(t)$ functions show a weak backscattering. Moreover for Lennard-Jones systems the differences are larger because of the less appropriate description of the binary term using a gaussian function.

Acknowledgments

The authors acknowledge Luis Enrique González, David González and Moises Silbert for helpful discussions and for providing us with the NPA pair potentials. We also thank Umberto Balucani for useful suggestions. Support from the DGICYT of Spain (Grant PB93-0971-C03) is also acknowledged.

References

[1] Boon J P and Yip S 1980 *Molecular Hydrodynamics* (New York: McGraw-Hill)
[2] Hansen J-P and McDonald I R 1986 *Theory of Simple Liquids* (London: Academic)
[3] Balucani U and Zoppi M 1994 *Dynamics of the Liquid State* (Oxford: Clarendon)
[4] Sjögren L and Sjölander A 1979 *J. Phys. C: Solid State Phys.* **12** 4369
[5] Sjölander A 1987 *Amorphous and Liquid Materials* ed E Lüscher *et al* (Dordrecht: Nijhoff)
[6] Schweizer K S 1989 *J. Chem. Phys.* **91** 5822
[7] Sjögren L and Sjölander A 1989 *Int. J. Quantum Chem.* **35** 851
[8] Sjögren L 1980 *J. Phys. C: Solid State Phys.* **13** 705
[9] Balucani U, Vallauri R, Gaskell T and Duffy S F 1990 *J. Phys.: Condens. Matter* **2** 5015
[10] Balucani U, Torcini A and Vallauri R 1992 *Phys. Rev.* A **46** 2159
Balucani U, Torcini A and Vallauri R 1993 *Phys. Rev.* B **47** 3011
[11] Shimojo F, Hoshino K and Watabe M 1994 *J. Phys. Soc. Japan* **63** 1821
[12] Balucani U, Torcini A, Stangl A and Morkel C 1993 *Phys. Scr.* T **57** 13
Balucani U, Torcini A, Stangl A and Morkel C 1996 *J. Non-Cryst. Solids* **205–207** 299
[13] Nowotny G and Kahl G 1996 *J. Non-Cryst. Solids* **205–207** 855
[14] Torcini A, Balucani U, de Jong P H K and Verkerk P 1995 *Phys. Rev.* E **51** 3126
[15] González L E, González D J and Canales M 1996 *Z. Phys.* B **100** 601
[16] Gudowski W, Dzugutov M and Larsson K E 1993 *Phys. Rev.* E **47** 1693
Gudowski W, Dzugutov M and Larsson K E 1993 *J. Non-Cryst. Solids* **156–158** 125
[17] Larsson K E 1994 *J. Phys.: Condens. Matter* **6** 2835
[18] Balucani U 1996 private communication
[19] Levesque D and Verlet L 1970 *Phys. Rev.* A **14** 408
[20] González L E, González D J, Silbert M and Alonso J A 1993 *J. Phys.: Condens. Matter* **5** 4283
[21] van der Lugt W and Albblas B P 1985 *Handbook of Thermodynamic and Transport Properties of Alkali Metals* ed R W Ohse (Oxford: Blackwell)
[22] Canales M, Padró J A, González L E and Giró A 1993 *J. Phys.: Condens. Matter* **5** 3095
[23] Canales M, González L E and Padró J A 1994 *Phys. Rev.* E **5** 3656
[24] Nowotny G, Kahl G and Hafner J 1995 *Phys. Scr.* T **57** 22
[25] Allen M P and Tildesley D J 1987 *Computer Simulation of Liquids* (Oxford: Clarendon)

[26] Beeman D 1976 *J. Comput. Phys.* **20** 130
[27] Berne B J and Harp G D 1970 *Adv. Chem. Phys.* **17** 216
[28] Söderström O, Dahlborg U and Gudowski W 1985 *J. Phys. F: Met. Phys.* **15** L23
[29] Vogelsang R and Hoheisel C 1989 *J. Stat. Phys.* **54** 315
Hoheisel C 1990 *Comput. Phys. Rep.* **12** 29
[30] Vallauri R and Bermejo F J 1995 *Phys. Rev.* E **51** 2654
[31] Verlet L 1968 *Phys. Rev.* **165** 201
[32] Zerah G 1985 *J. Comput. Phys.* **61** 280
[33] Schoen M, Vogelsang R and Hoheisel C 1986 *Mol. Phys.* **57** 445
[34] Hoheisel C and Vogelsang R 1988 *Comput. Phys. Rep.* **8** 1
[35] Press W H, Flannery B P, Teukolsky S A and Vetterling W T 1989 *Numerical Recipes* (New York: Cambridge University Press)
[36] Lovesey S W 1971 *J. Phys. C: Solid State Phys.* **4** 3057
[37] Hoshino K, Ugawa H and Watabe M 1992 *J. Phys. Soc. Japan* **61** 2182
[38] González D J, González L E and Hoshino K 1994 *J. Phys.: Condens. Matter* **6** 3849